ELSEVIER

Int. J. Miner. Process. 69 (2003) 29–47

INTERNATIONAL JOURNAL OF MINERAL PROCESSING

www.elsevier.com/locate/ijminpro

The effect of slurry rheology on fine grinding in a laboratory ball mill

C. Tangsathitkulchai*

School of Chemical Engineering, Institute of Engineering, Suranaree University of Technology, III University Avenue, Muang District, Nakhon Ratchasima 30000, Thailand

Received 19 December 2001; received in revised form 6 May 2002; accepted 7 May 2002

Abstract

The kinetics of slowing down of breakage rates for fine wet grinding of 20×30 mesh quartz fraction was investigated as a function of slurry concentration in a laboratory batch ball mill. It was discovered that the slowing-down effect occurred to all particle sizes in the charge and at any slurry concentrations even for very dilute conditions. The slowing-down factor was defined and showed good correlation with the relative apparent viscosity of the slurry. Three different grinding regimes in fine grinding region were identified with reference to their rheological behavior. Hypotheses for the mechanisms of slowing-down effect were also given.

Keywords: fine wet grinding; ball mill; slurry rheology; breakage rates

1. Introduction

It is generally observed that dry and wet grinding of materials in tumbling ball mills to very fine sizes can lead to the slowing down of the overall grinding process (Austin et al., 1984; Frances and Laguerie, 1998; Yekeler et al., 2001). This effect signifies that ball–ball collision in the grinding region cannot transmit sufficient stress to fracture individual particles as fines accumulate beyond a certain level. Austin and Bagga (1981) postulated that the slowing down of grinding rates observed in the dry systems could

* Tel.: +66-44-224490; fax: +66-44-224220.
E-mail address: chaiyot@ccs.sut.ac.th (C. Tangsathitkulchai).

0301-7516/03/$ - see front matter © 2003 Elsevier Science B.V. All rights reserved.
PII: S0301-7516(02)00061-3

result from the inefficiency of particle capture by grinding media, caused by the ability of the cohesive fine particles to flow away from the ball collision zone. Tangsathitkulchai and Austin (1989) studied extensively the effect of slurry density on wet grinding behavior in a laboratory ball mill. For the process of fine wet grinding, they found the slowing down of particle breakage to occur at any slurry concentrations, even for dilute pulps of low viscosities. In addition, the changes in slurry concentration and particle size distribution, which had a direct effect on the rheological character of the slurry, was found to alter the circulation path of the ball charge and thus the interaction between the particles and the grinding media. The overall effect gave rise to the existence of various grinding regimes relevant to wet ball milling. From these results, it is clear that the basic mechanisms associated with the breakage process and the slowing down of breakage rates in particular are complex, possibly being influenced largely by the viscous nature of the slurry pulp.

The significance of fine wet grinding in many industrial applications is obvious, but available data in this area are quite limited. This paper reports further results on the kinetic analysis and mechanisms underlying the slowing down of breakage rates in fine wet grinding, with emphasis on the effect of slurry rheology in a batch laboratory ball mill.

Table 1
Mill characteristics and grinding conditions

Mill	
Inside diameter (m)	0.20
Length (m)	0.175
Internal volume (m^3)	5.2×10^{-3}
Running speed (rpm)	76
Critical speed (rpm)	108
Fraction of critical speed (ϕ_c)	0.70
Lifters	
Cross-section	Semicircular
Diameter (m)	2×10^{-2}
Numbers	6
Grinding media	
Material	Alloy steel balls
Diameter (m)	2.54×10^{-2}
Density (kg m^{-3})	7.8×10^3
Ball filling, as fractional mill volume occupied by ball bed (J)	0.30
Total ball weight (kg)	7.72
Number of balls	115
Powder charge	
Material	Crystalline quartz
Density (kg m^{-3})	2.65×10^3
Particle size	20×30 mesh (850×600 μm)
Total weight (kg)	1.05
Powder filling, as volume fraction of ball bed voidage (U)	1.0
Slurry concentration (vol.% solid)	20–65

2. Experimental

2.1. Materials

The material used in this study was white crystalline quartz from North Carolina. Spectrochemical analysis showed the quartz to contain less than 1% of combined Co, Fe and Al. Large lumps of the raw material were staged crushed in jaw and roll crushers to obtain a -8 mesh discharge. The crushed product was separated into different sieve fractions and the 20×30 mesh size fraction was kept for further grinding tests.

2.2. Mill and test conditions

Batch grinding tests were conducted in a steel laboratory cylindrical mill, fitted with six equally spaced lifters to key the ball charge to give proper ball tumbling action. On one end of the mill was a detachable steel plate with attached rubber ring to seal the mill compartment. The grinding media used were chrome alloy steel balls. Table 1 lists the mill characteristics and grinding conditions used in this study.

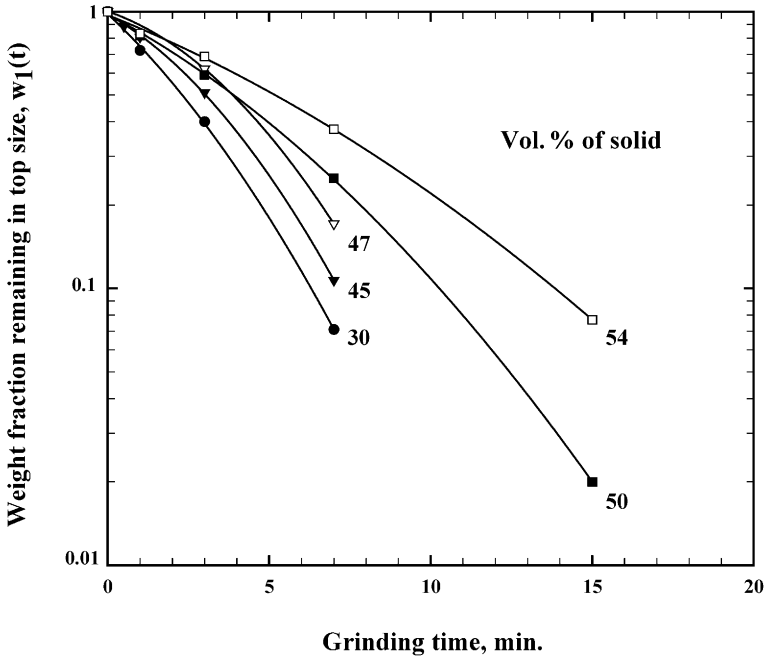

Fig. 1. First-order plots for wet grinding of 20×30 mesh quartz at various slurry concentrations ($J = 0.3$, $U = 1.0$, $\phi_c = 0.70$).

2.3. Test procedure

The mill was first charged with certain amounts of grinding balls. Next, the 20 × 30 mesh quartz feed was loaded into the mill and the measured volume of distilled water was poured in to obtain the required solid concentration in the slurry. The mill was then sealed and rotated on a roller table for a set period of time. After the grinding was completed, the mill content was emptied on a retaining steel grid to separate the balls and the product slurry. The slurry was filtered and the cake was dried in an electric oven.

Agglomerates in the dried product were broken up, mixed from corner to corner and randomly sampled to obtain a sample weight of 30–80 g depending on the fineness of grinding. The weighted materials were then wet screened on a 400 mesh sieve to reduce screen blinding. The screen was dried in the oven at 150 °C for about 3 h. The plus 400 mesh material was weighed and sieved with a nest of 200 mm screens arranged in a sequence down to 400 mesh for 20 min on the Rotap shaking device. The sieve analysis of the product was computed based on the recorded weights of material retained on each screen and in the bottom pan. The −400 mesh particles collected from wet sieving were filtered, dried and kept for further subsieve analysis using Microtrac laser diffraction instrument (Model 7991-01, Leeds and Northrup).

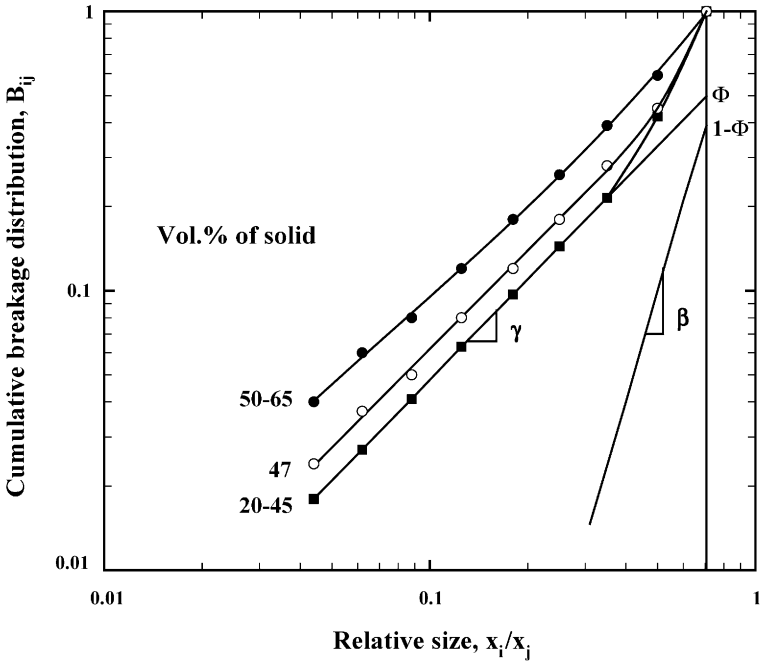

Fig. 2. Primary breakage distribution function for wet grinding of 20 × 30 mesh quartz feed (J = 0.3, U = 1.0, ϕ_c = 0.70).

3. Results and discussion

3.1. Analysis of fine wet grinding

The forward computation of product size distributions for batch grinding can be performed based on the well-known batch grinding kinetic model (Austin et al., 1984; Austin, 1999). The model equation in discrete form reads

$$\mathrm{d}w_i(t)/\mathrm{d}t = -S_i w_i(t) + \sum_{j=1}^{i-1} b_{ij} S_j w_j(t), \quad n \geq i \geq j, \tag{1}$$

where t is the time of grinding, n is the number of size intervals, w_i is the weight fraction of particles of screen size i, S_i is a constant termed the specific rate of breakage of size i and b_{ij} is the primary daughter fragments defined as the weight fraction of broken products from size interval j, which appears in size range i on primary fracture. In cumulative form, the primary breakage distribution can be expressed as

$$B_{ij} = \sum_{k=n}^{i} b_{kj}, \tag{2}$$

where B_{ij} is the sum fraction of material broken out from size j that falls less than the upper size of interval i. The solution of Eq. (1) for a set of n differential equations gives

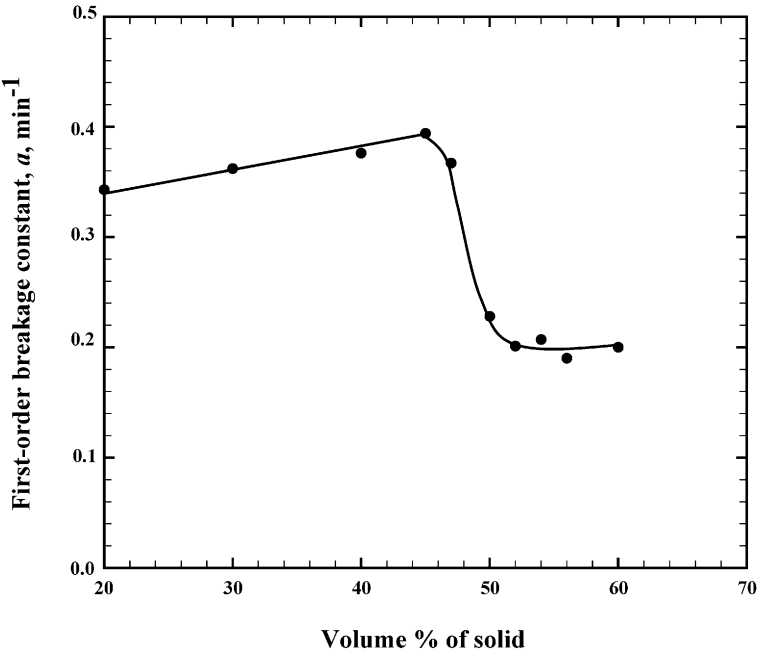

Fig. 3. Dependence of breakage constant, a, on slurry concentration (20×30 mesh quartz, $J = 0.30$, $U = 1.0$, $\phi_c = 0.70$).

prediction of product size distributions at various grinding times, given a starting feed size $w_i(0)$ and the two breakage parameters (S_i and B_{ij}), which require experimental determination. For the breakage of top size material (size 1), integration of Eq. (1) gives

$$w_1(t) = w_1(0)\exp(-S_1 t). \tag{3}$$

Therefore, if a plot of log $w_1(t)$ versus t gives a straight line, grinding is said to be first order and S_1 is determined from the slope of the line. Any deviation from the linear relationship on such a plot indicates non-first-order grinding and the instantaneous specific breakage rate of the top size can be deduced from Eq. (3) as

$$S_1(t) = \frac{-\mathrm{d}}{\mathrm{d}t}\ln[w_1(t)/w_1(0)]. \tag{4}$$

It was found that the forward simulation for wet grinding 20 × 30 mesh quartz fraction using the first-order concept previously discussed was complicated by the non-first-order breakage behavior of this starting feed size. Fig. 1 shows typical disappearance kinetic plots for grinding 20 × 30 mesh quartz at various slurry concentrations. It is clear that the breakage exhibits a non-first-order acceleration in the specific breakage rate (increasing slope of the curve) with the time of grinding. As reported by Tangsathitkulchai and Austin (1989) and recently by Tangsathitkulchai (2002), this rate acceleration appeared to occur predominantly with the top size material and the degree of this acceleration effect tended to diminish as the next smaller size became the new top size in the charge. Therefore, it

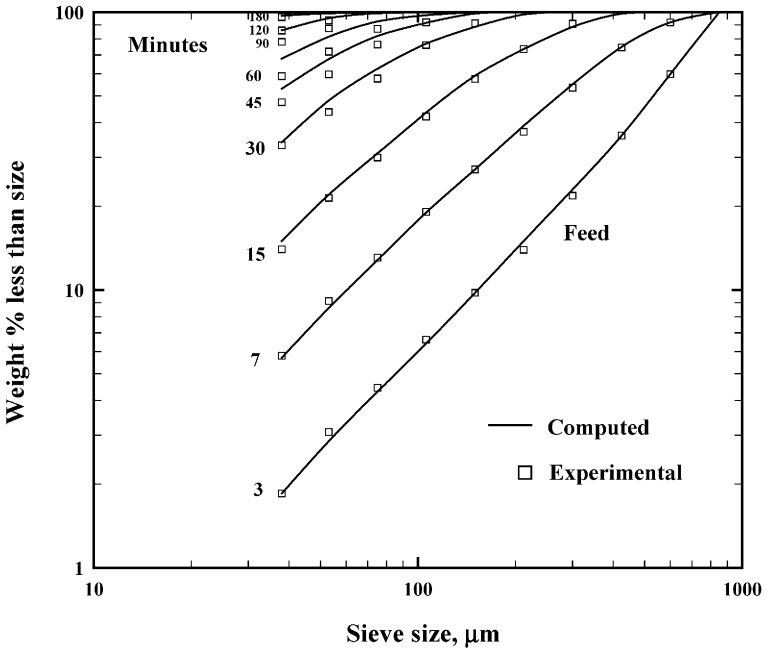

Fig. 4. Comparison of computed and experimental size distributions, showing the slowing down of breakage rate at long grinding times (quartz, $J = 0.3$, $U = 1.0$, $\phi_c = 0.70$, 40% solid by volume).

may be reasoned that after a period of grinding so that the quantity of the initial top size present is relatively small, the overall grinding process may be treated as first order without appreciable error. Breakage rates in this normal size consist which are of interest and hence need to be characterized.

Based on the above discussion, the forward computation algorithm for wet grinding of a monosize feed of 20 × 30 mesh quartz was achieved as follows. A short-time product size distribution, say 1 min grinding time of the initial feed size, was used as a starting feed ($t=0$) and assuming constant rates of breakage for all sizes except the top size. S_1 values for the top size were determined from the disappearance kinetic plot of Fig. 1 over the range from 1 min on. For smaller size fractions, their specific rates of breakage followed the usual functional relation:

$$S_i = a(x_i/x_o)^{\alpha}, \tag{5}$$

where x_i is the particle size (mm), x_o is a reference size (1 mm), $\alpha=0.80$ for quartz material and a is the first-order breakage constant, being a function of slurry concentration. Fig. 2 shows the primary breakage distribution using the BII method (Tangsathitkulchai and Austin, 1985). These curves can be fitted by the sum of two power functions of the form

$$B_{ij} = \Phi_j(x_{i-1}/x_j)^{\gamma} + (1-\Phi_j)(x_{i-1}/x_j)^{\beta}. \tag{6}$$

Next, the batch grinding equation was solved by a trial-and-error search procedure to estimate the parameter a, which gave a one-point match for a percentage passing 200 mesh (75 μm) between the simulated and the experimental size distributions.

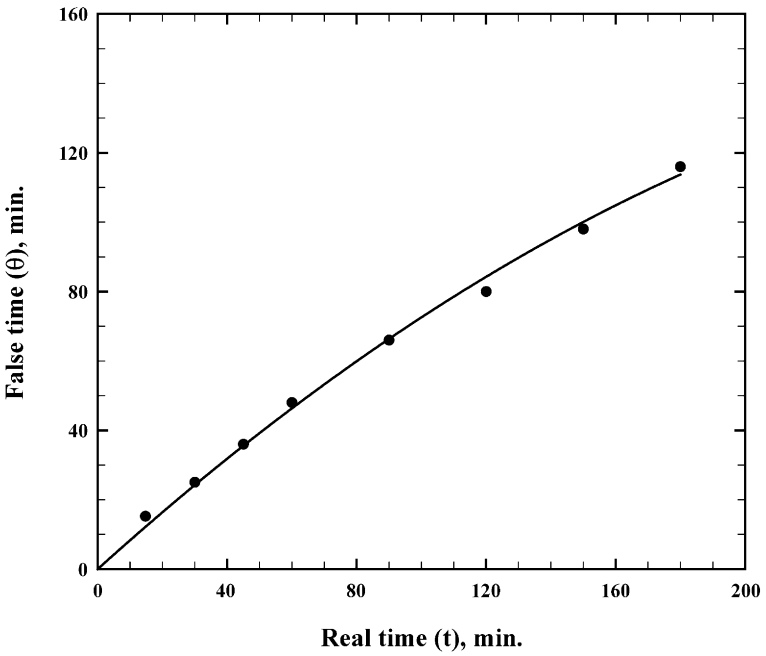

Fig. 5. False time (θ) versus real grinding time (t) (20 × 30 mesh quartz feed, $J=0.3$, $U=1.0$, $\phi_c=0.70$, 40% solid by volume).

Fig. 3 shows the effect of slurry concentration on the computed first-order breakage constant, a, with a maximum in grinding rate occurring around 45 vol.% solid concentration. Fig. 4 compares the computed and experimental size distributions for grinding at 40 vol.% solid concentration based on the first-order hypothesis. For grinding times less than 30 min or up to the fineness of about 80% passing 100 μm, the agreement of size distributions is excellent. However, at longer grinding times, the simulation tends to overpredict the experimental results and the discrepancy seems to increase with increasing times. This difference appears to indicate that the whole grinding process starts to slow down when enough fine materials accumulate in the mill charge, possibly caused by some changes in the breakage mechanisms. The rate analysis in this fine grinding region was achieved by using the false-time technique proposed by Austin and Bagga (1981). In brief, the slowing down of breakage is assumed to be uniform for all particle sizes and the values of S_i at grinding time t can be represented by

$$S_i(t) = K_s S_i(0), \quad K_s \leq 1, \tag{7}$$

where $S_i(0)$ is the set of normal first-order S values and K_s is a slowing-down factor, being a function of fineness of grinding. If the B and α values are assumed to be constant, the solution of the batch grinding equation can still give the correct predicted size distribu-

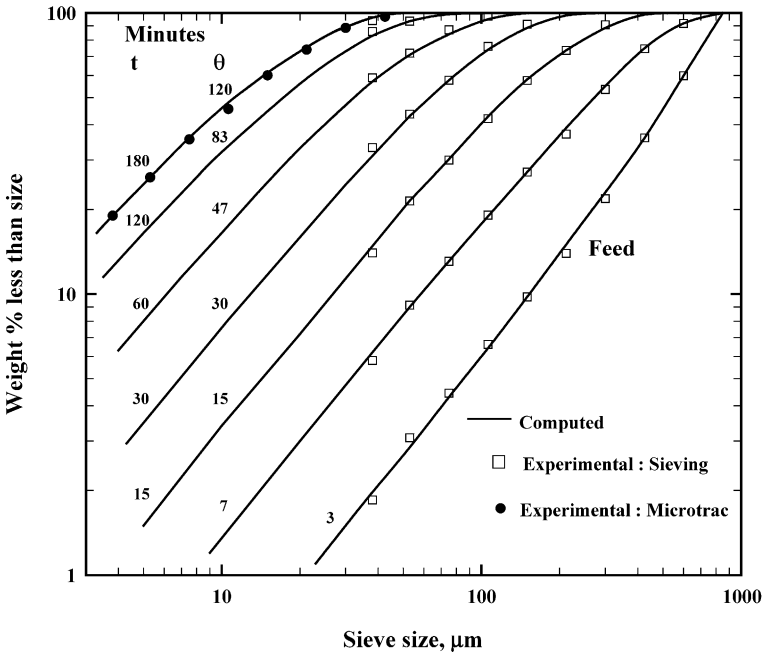

Fig. 6. Experimental versus computed size distributions using false-time concept for quartz wet ground in water ($J=0.30$, $U=1.0$, $\phi_c=0.70$, 40% solid by volume).

tions, but a false time (θ) has to be used in the computation. The slowing-down factor, K_s, is related to θ and t by

$$K_s = d\theta/dt. \tag{8}$$

The K_s value is unity in the normal first-order region but decreases as the rate is slowing down. The false time can be estimated by running the grinding simulation to give a match to a specified point on the product size distribution, for example, the percentage of material less than 270 mesh. Fig. 5 shows the relation between the false time and the actual time of grinding. Fig. 6 demonstrates that the sieve size distributions in the slowing-down region can be predicted with reasonable accuracy using the false-time concept. Also shown at the longest grinding time is the size distributions in the subsieve region obtained by correcting the Microtrac sizes to the equivalent sieve sizes using the procedure developed by Austin and Shah (1983).

Fig. 7 shows the values of K_s as a function of 80% passing size, x_{80}, for a range of slurry concentrations. In general, the grinding first proceeds at normal first-order rate ($K_s = 1$) until the size consist reaches a critical 80% passing size, designated as x^*_{80}, then the rate starts to fall continuously with increasing fineness of grinding. This x^*_{80} appears to occur at much larger values for very dense slurries of 60% and 65% solid by volume,

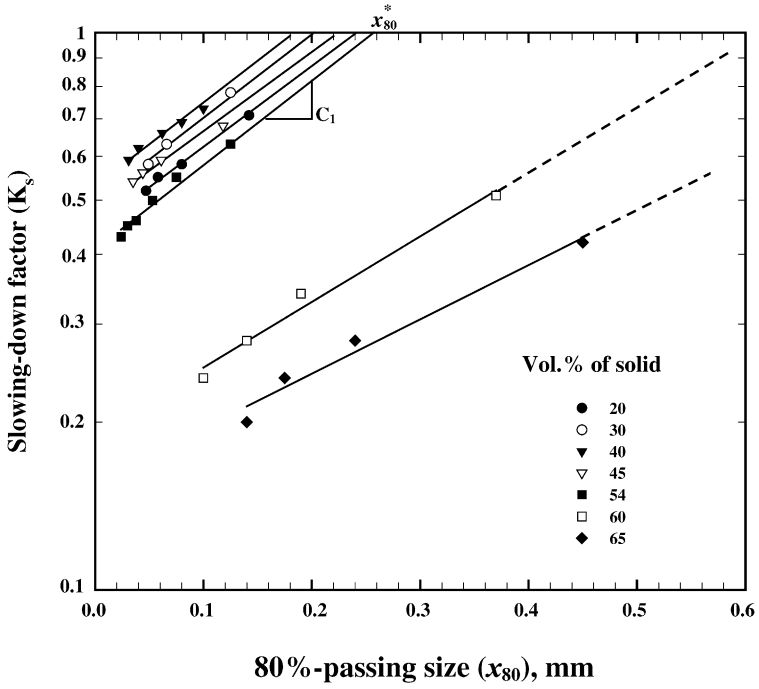

Fig. 7. Slowing-down factor as a function of 80% passing size for various slurry concentrations (quartz feed, $J = 0.3$, $U = 1.0$, $\phi_c = 0.70$).

indicating a dramatic drop in the breakage action by the grinding media. Fig. 8 illustrates further that a slurry having a higher normal first-order rate can be ground to a finer size before the onset of the slowing-down effect. The abrupt change in the slope of the curve, which occurs at 54 vol.% solid concentration, is further indicative of the difference in breakage mechanisms between grinding in the low and high slurry concentration regions. The linear relation between K_s and x_{80} as shown in Fig. 7 can be represented by the equation:

$$K_s = \exp[C_1(x_{80} - x_{80}^*)/x_0], \quad x_{80} \leq x_{80}^*, \tag{9}$$

where C_1 is a constant determined from the slope of the curve and is a function of slurry concentration, as shown in Fig. 9. It is interesting to observe from Fig. 7 that if the slurry concentration is not too viscous to interrupt the ball tumbling action, that is, less than 54 vol.% solid concentration, the values of C_1 are almost constant, being insensitive to the change in slurry concentration. To obtain further useful results, the determination of slowing-down factor should be extended to cover the effects of mill operating conditions such as ball size, mill diameter, ball and powder filling level and mill speed. The incorporation of quantitative description of this slowing-down effect into a mill model should be useful for the improvement of mill circuit design capability.

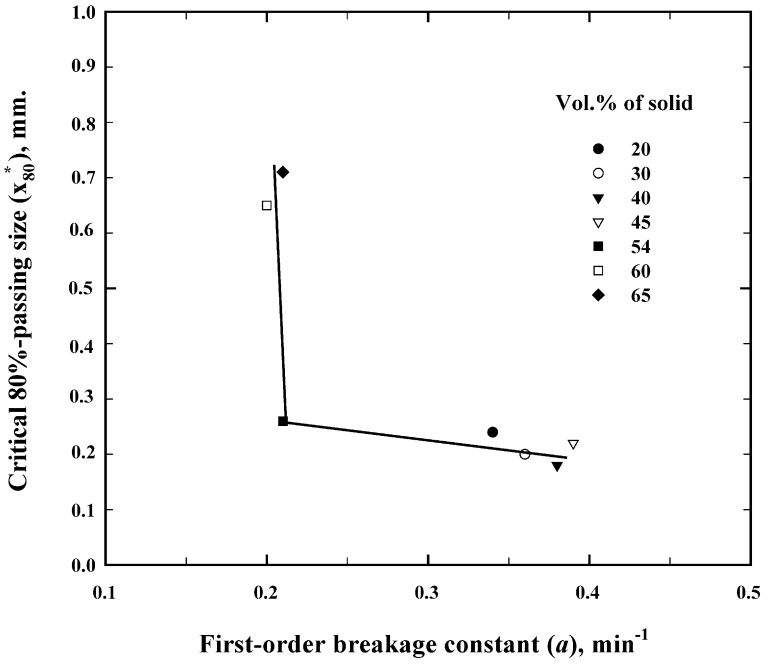

Fig. 8. Relation between first-order breakage constant, a, and 80% passing size at the onset of slowing-down effect (x_{80}^*).

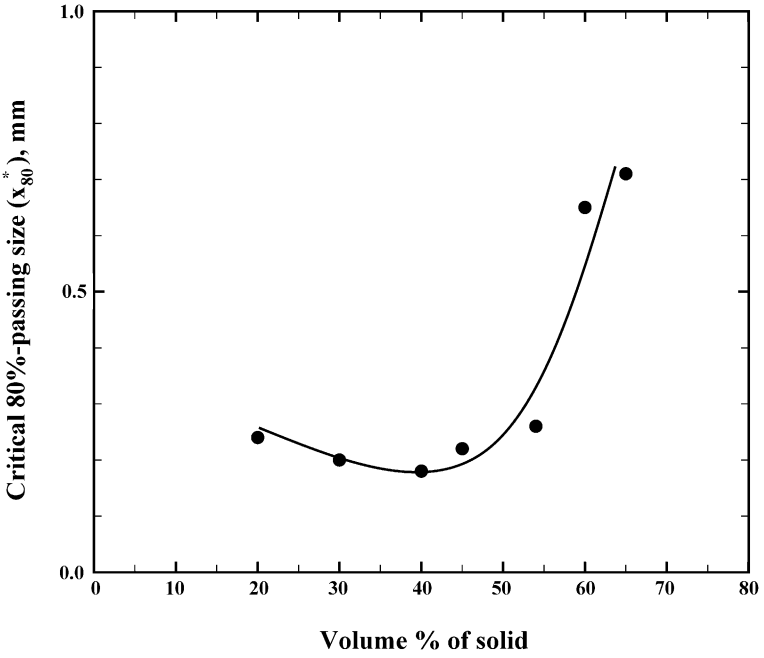

Fig. 9. Variation of x^*_{80} with slurry concentration (20 × 30 mesh quartz feed, $J = 0.3$, $U = 1.0$, $\phi_c = 0.70$).

3.2. Rheological effect in fine wet grinding

The work of Tangsathitkulchai and Austin (1988) has shown that homogeneous slurries of particles produced by ball mill grinding exhibited a time-independent non-Newtonian behavior of *pseudoplastic with and without yield stress followed by Bingham plasticity.* This type of rheological behavior is exemplified by Fig. 10 for quartz slurries of a set of size distribution as a function of volume percent solid. It appears that the transition of flow character from pseudoplasticity to Bingham plasticity occurs at a shear rate around 30 s^{-1}. The basic equation used to describe the rheological data was given by

$$\frac{\tau}{\mu_L} = \frac{\tau_Y}{\mu_L} + \left[\frac{\tau_{BY}}{\mu_L} + \frac{\mu_{PL}}{\mu_L}\frac{dv}{dy} - \frac{\tau_Y}{\mu_L}\right]Q, \tag{10}$$

where τ is shear stress, dv/dy is shear rate, τ_Y is true yield stress, τ_{BY} is Bingham yield stress, μ_{PL} is Bingham plastic viscosity, μ_L is suspending liquid viscosity, and Q is a function that accounts for pseudoplastic behavior at low shear rates. In terms of relative apparent viscosity, Eq. (10) can be expressed as

$$\frac{\mu_a}{\mu_L} = \left[\frac{\tau_Y}{\mu_L} + \left[\frac{\tau_{BY}}{\mu_L} + \frac{\mu_{PL}}{\mu_L}\frac{dv}{dy} - \frac{\tau_Y}{\mu_L}\right]Q\right](dv/dy)^{-1}, \tag{11}$$

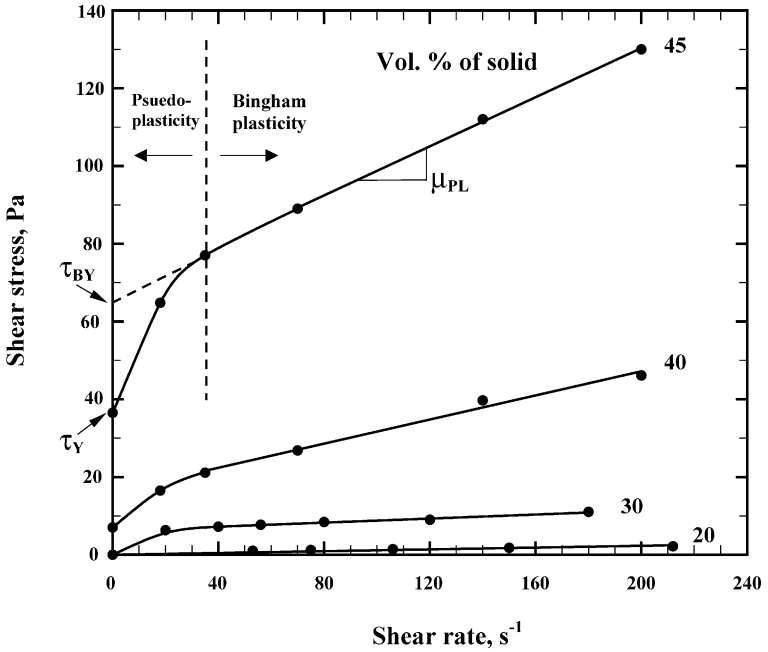

Fig. 10. Typical shear stress versus shear rate for quartz slurries as a function of slurry concentration (Rosin–Rammler distribution modulus, 1.22; Rosin–Rammler size modulus, 29 μm; liquid s.g., 2.63; liquid viscosity, 0.0028 Pa s).

where μ_a is the apparent viscosity, being the ratio of shear stress and shear rate. The function Q was approximated by an empirical equation:

$$Q = 1 - \exp\Big[- 0.32(\mathrm{d}v/\mathrm{d}y)^{0.72} \Big]. \tag{12}$$

The remaining rheological parameters were represented by the following correlations:

$$\frac{\tau_Y}{\mu_L} = (6500/k)^{4.48C^{1.35}} \tag{13}$$

$$\frac{\tau_{BY}}{\mu_L} = 135(1000/k)^{6C^{2.1}} \tag{14}$$

$$\log\left[\frac{\mu_{PL}}{\mu_L}\right] = \left[4.26 + \frac{1}{1 + \left[\frac{0.06}{(m-0.7)^2}\right]^{4.7}}\right]\left[\frac{C}{1-C}\right]^{1.1+\exp(-14.2m^{2.6})}[k]^{-0.21} \tag{15}$$

where C is volume fraction of solid in slurry and k and m are the size modulus and distribution modulus of the fitted Rosin–Rammler size distribution equation, respectively.

The proposed correlations covered the following range of variables: $C = 0.20-0.65$, $k = 10-200$ μm, $m = 0.40-1.20$, and $dv/dy = 0-200\ s^{-1}$.

The rheological properties of slurries in the slowing-down region were estimated using the empirical equations developed by Tangsathitkulchai and Austin (1988), as mentioned above. Three distinct regimes of rheological behavior can be identified in relation to the change in slurry concentration range. Fig. 11 shows the results. In Regime I of low concentrations (20 vol.% solid), the slurry exhibits almost no yield stress values and rheological character resembles that of Newtonian fluids (see Fig. 11a). Regime II of

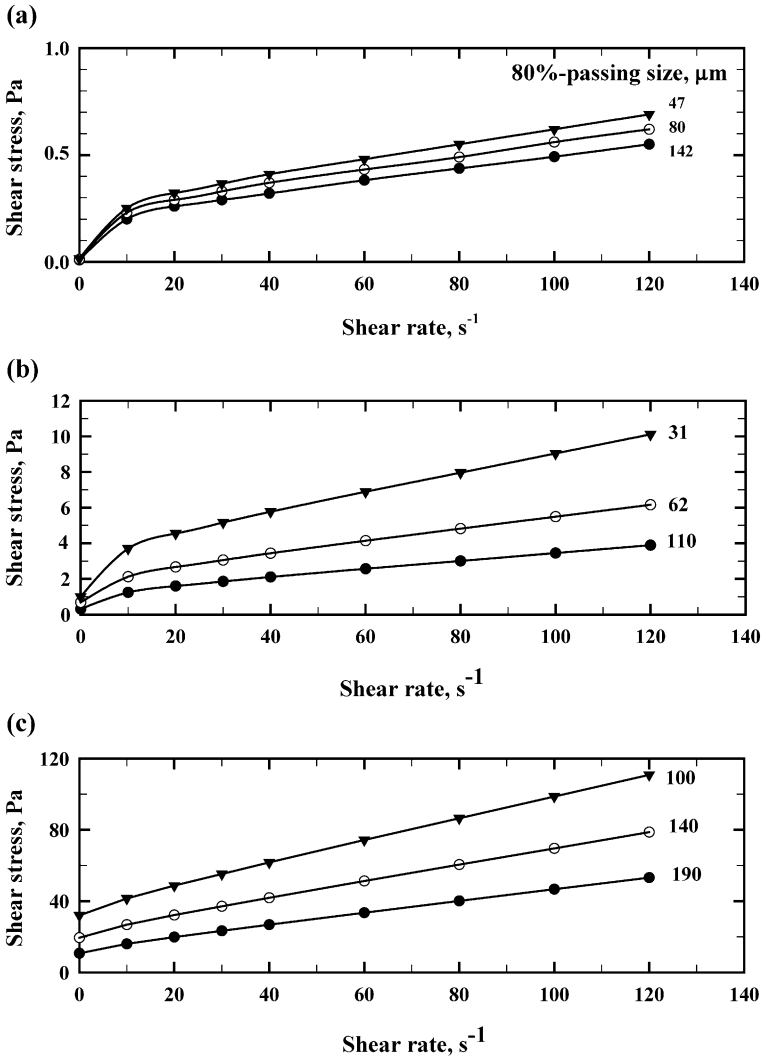

Fig. 11. Rheological character of slurries in the slowing-down region for various volume percent solid and fineness of grinding: (a) 20%, (b) 40% and (c) 60%.

normal concentrations (30–45 vol.% solid) possesses some yield stresses and a rheological character of pseudoplastic followed by Bingham plastic behavior (see Fig. 11b). Regime III of high slurry concentrations (54–65 vol.% solid) is typified by substantial yield stresses and a true Bingham plastic behavior (see Fig. 11c). Figs. 12–14 shows the effect of 80% passing size of product slurry on the three rheological parameters τ_Y, τ_{BY}, and μ_{PL}, respectively. Similar trends are observed in that the values of these parameters increase with increasing fineness (decreasing 80% passing size) and the degree of increase (slope of the curve) is more pronounced at higher slurry concentrations, except for dense slurries at 60 and 65 vol.% solid that show much flatter slopes. Table 2 lists the approximate range of rheological parameters for the three rheological regimes encountered in fine wet grinding, as previously mentioned.

To check the effect of slurry rheology on the slowing down of breakage rates in fine wet grinding, the slowing-down factor (K_s) was plotted against the relative apparent viscosity of slurry (μ_R) on a log–log scale, as shown in Fig. 15. It should be noted that μ_R is the ratio between the slurry apparent viscosity (μ_a) and the viscosity of suspending medium (μ_L), with μ_a being evaluated at an arbitrary shear rate of 100 s^{-1}. In general, the slowing-down factor starts from the value of unity at relatively low viscosities, corresponding to the first-order grinding. When a critical relative viscosity, μ_R^*, is reached, the value of K_s starts to decline and falls in a linear fashion after the slurry viscosity is further increased. The degree of this decrease (slope of the curve) becomes less as the slurry concentration is increased, except for slurries at 60% and 65% solid by volume where the slope starts to

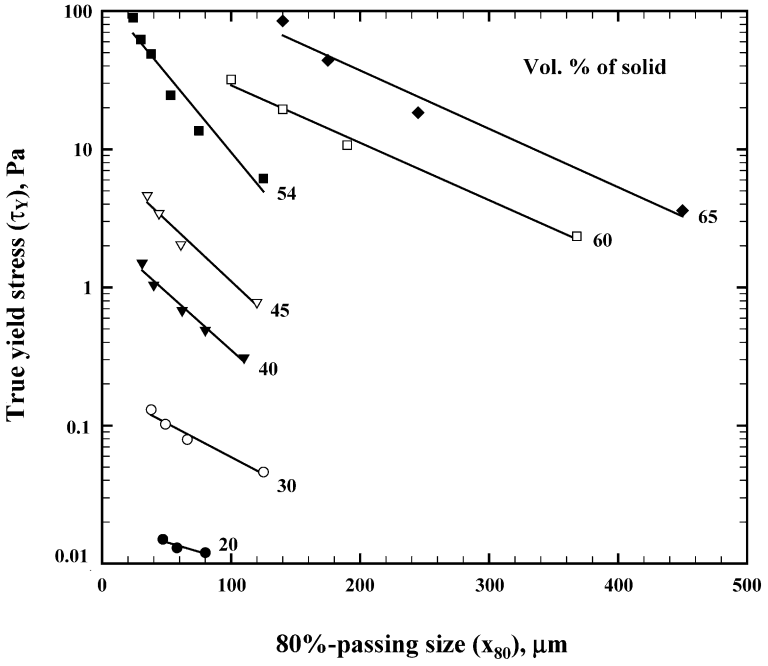

Fig. 12. Effect of 80% passing size, x_{80}, on the true yield stress, τ_Y.

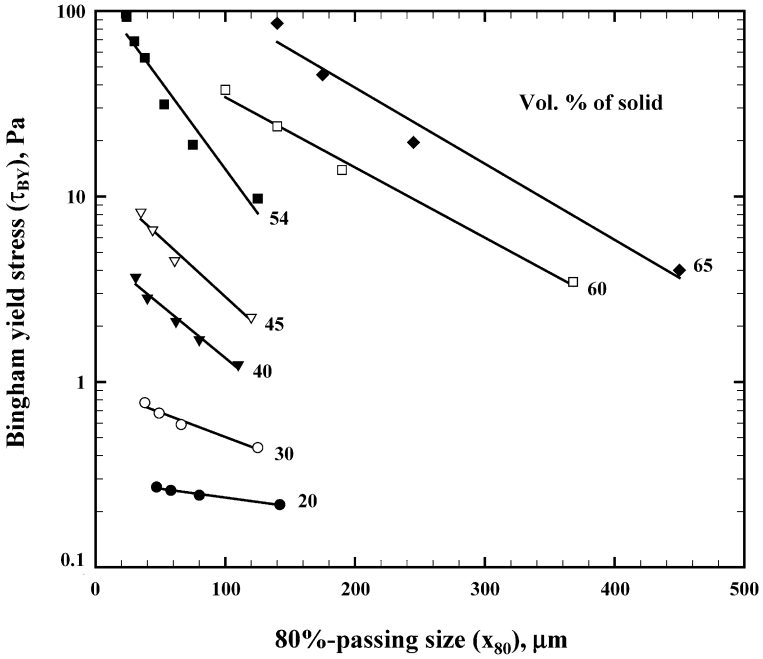

Fig. 13. Effect of 80% passing size, x_{80}, on the Bingham yield stress, τ_{BY}.

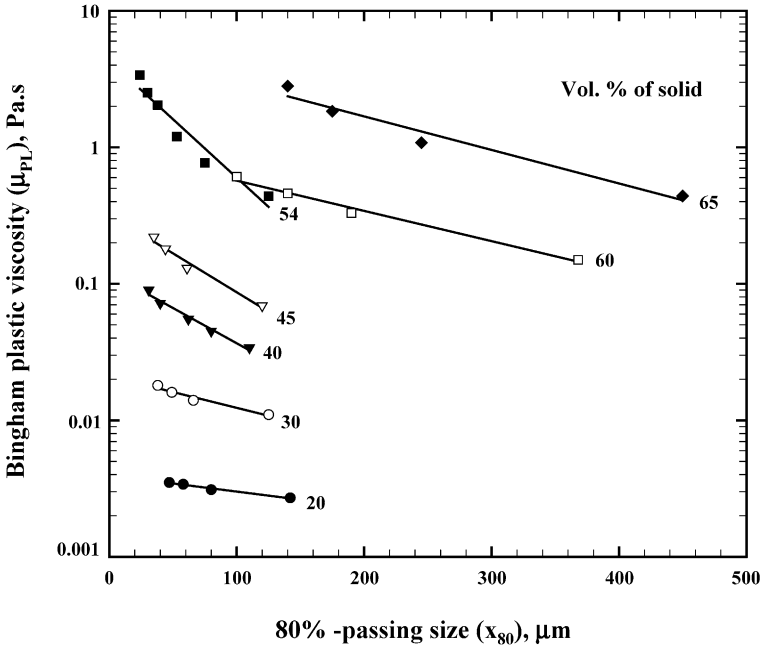

Fig. 14. Effect of 80% passing size, x_{80}, on the Bingham plastic viscosity, μ_{PL}.

Table 2
Classification of grinding regimes in the slowing-down region of fine wet grinding based on ranges of rheological parameters (20×30 mesh quartz ground in water, $J=0.3$, $U=1.0$, $\phi_c=0.70$)

Regime	Slurry concentration (vol.% solid)	80% passing size (x_{80}) (μm)	True yield stress (τ_Y) (Pa)	Bingham yield stress (τ_{BY}) (Pa)	Plastic viscosity (μ_{PL}) (Pa s)
I	20	47–142	0.01–0.02	0.2–0.3	0.002–0.004
II	30–45	30–130	0.05–5.0	0.5–10.0	0.006–0.20
III	54–65	25–450	5.0–100	10.0–100	0.20–3.0

increase again. It is interesting to notice further that the K_s versus μ_R curves can be separated into three different groups, coinciding with the three slurry regimes as discussed previously. These results tend to suggest that the mechanisms associated with the slowing-down effect in each regime are definitely different. The quantitative relationship between slowing-down factor and slurry viscosity can be conveniently expressed as

$$K_s = \left(\frac{\mu_R}{\mu_R^*}\right)^{C_2}, \quad \mu_R \geq \mu_R^*, \tag{16}$$

where C_2 is a constant, depending on slurry concentration as shown in Fig. 16, and the values of μ_R^* are 3.8, 8.7 and 40 for grinding in Regime I (20 vol.% solid), Regime II (30–45 vol.% solid) and Regime III (54–65 vol.% solid), respectively.

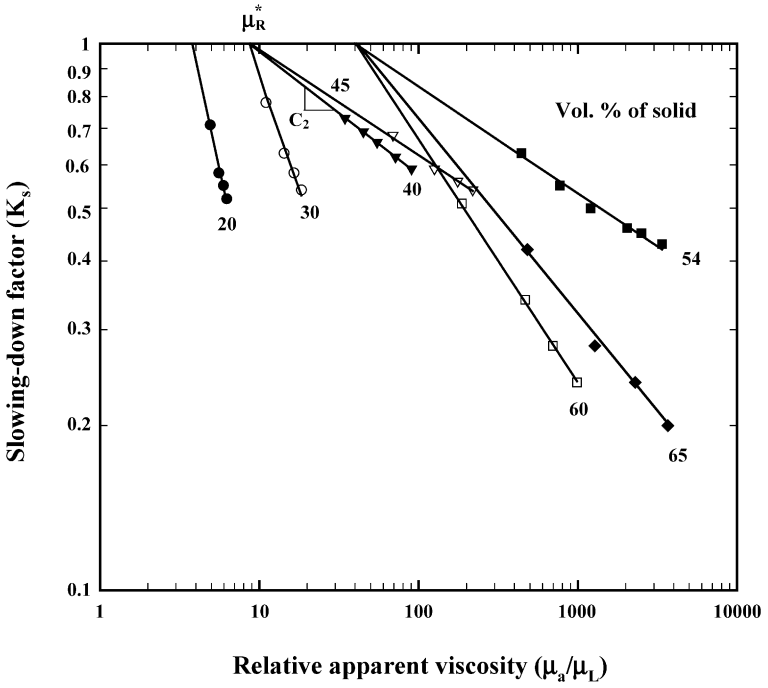

Fig. 15. Effect of relative viscosity of slurry on the slowing-down factor [shear rate, 100 s^{-1}; liquid viscosity (μ_L), 0.001 Pa s].

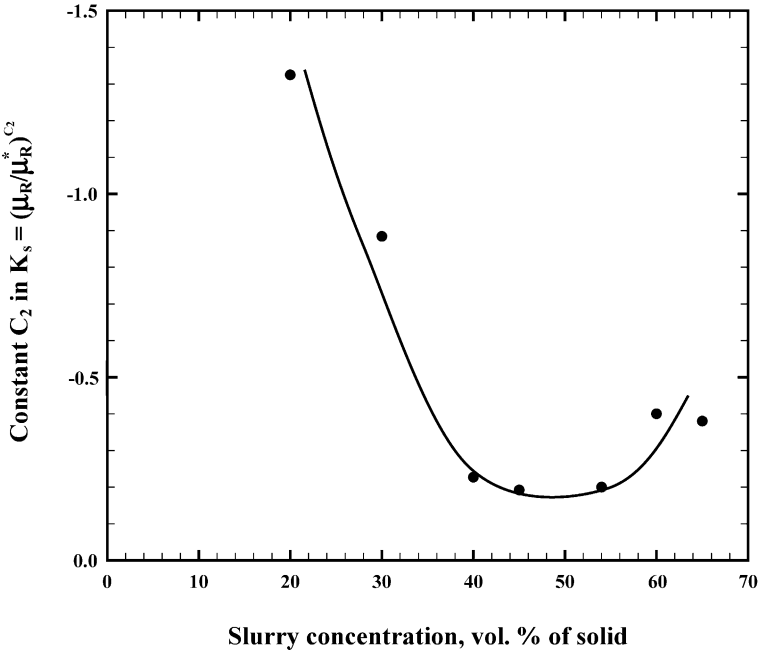

Fig. 16. Dependence of constant C_2 in $K_s=(\mu_R/\mu_R^*)^{C_2}$ on slurry concentration.

To further understand the mechanisms involved in the slowing down of breakage rates in fine wet grinding, the measurement of mill power and the visual observation of rotating mill charge through a transparent plastic end plate were carried out. Fig. 17 shows the variation of net mill power as a function of grinding time in the slowing-down region. For the concentration range of 20–54 vol.% solid, the net mill power draw remained substantially constant, indicating good ball tumbling action throughout the grinding operation. There was an indication from visual observation that the variation in the magnitude of mill power draw with slurry concentration corresponded closely to the change in the lifting height of the ball mass. This observation implies that the primary effect of slurry viscosity is to influence the friction between moving ball layers and between a ball layer and a mill wall. On the other hand, grinding at high slurry concentrations of 60 and 65 vol.% solid was associated with the continuous reduction in mill power. This drop was due principally to the ability of the thick pulps to hold the grinding media together and to the mill wall, thus leaving less active balls available for the breakage process in the cascading zones.

Therefore, it is clear that the slowing down of grinding rates in Regime III at high slurry concentrations occurs simply from the highly viscous nature of the slurry that can interrupt the smooth rolling and effective collision of the grinding media. However, it is not easy to explain the mechanism of slowing-down effect for more dilute pulps (<60 vol.% solid) because there was no change in the mill power. For Regime I of very dilute slurries (20 vol.% solid or less), the slowing-down mechanism could involve the displacement of fine particles from the point of contact caused by fluid drag as grinding balls approaching each

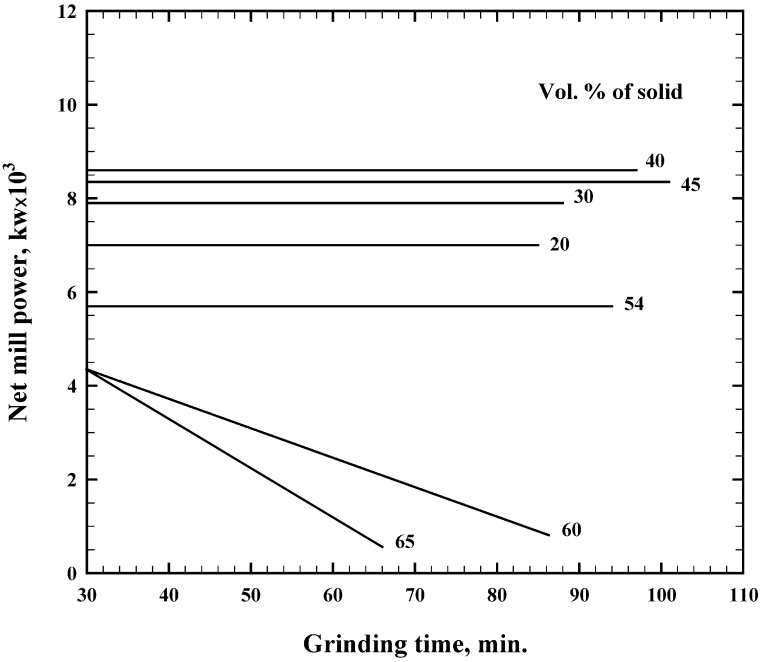

Fig. 17. Net mill power as a function of time for wet grinding in the slowing-down region (20 × 30 mesh quartz ground in water, $J = 0.3$, $U = 1.0$, $\phi_c = 0.70$).

other, whereby reducing the efficiency of particle capture by the grinding media. It may be argued that this hydrodynamic effect could be counteracted by the increased viscosity of the slurry as particles becoming finer. However, this countereffect may be less significant due to the insensitivity of viscosity change with the fineness of particle sizes for this low concentration range. In addition, the highly turbulent state of slurry will, to a certain extent, keep most particles in suspension, thus further preventing them from getting access to the grinding zones. For grinding in Regime II of normal slurry concentrations (30–45 vol.% solid), the coating of wet slurry on the grinding surfaces was observed and believed to be the responsible factor for the slowing down of breakage rates in this region. That is, as grinding proceeds, the thickness of the coated particle layer on the ball surfaces increases, resulting in the lowering of the intensity of ball impacts and hence reducing the efficiency of energy transmission by balls to fractured particles.

4. Conclusions

When the first-order kinetic analysis of batch grinding of 20 × 30 mesh quartz was extended to fine grinding region, using the same set of breakage parameters, the decrease in specific breakage rates was observed for all particle sizes in the mill. This slowing-down effect appeared to occur for any slurry concentrations, even for dilute slurries of low

viscosities in nature. The simulation of product size distributions in the slowing-down region was successfully achieved through the application of a false-time method that led to the introduction of a slowing-down factor as a quantitative measure for the slowing down in breakage rates. For fine grinding region, three slurry regimes of different concentration range can be identified with respect to their rheological behavior, namely Regime I of low slurry concentrations (20 vol.% solid or less) with characteristic of Newtonian-like behavior, Regime II of normal slurry concentrations (30–40 vol.% solid) with combined pseudoplastic/Bingham plastic character and Regime III of high slurry concentrations (54–65 vol.% solid) showing Bingham plastic property of substantial yield stresses. The slowing-down factor when correlated with the relative viscosity of the slurry could be separated into three different groups that matched exactly with the three identified slurry regimes. Mechanisms of slowing-down effect in fine wet grinding were hypothesized to involve the different roles of slurry rheology in different grinding regimes. They are reduction of particle capture efficiency due to fluid drag for Regime I, reduced efficiency of stress transmission due to ball coating by particle layer for Regime II and reduction of ball collision frequency due to ball adherence for Regime III.

References

Austin, L.G., 1999. A discussion of equations for the analysis of batch grinding data. Powder Technol. 106, 71–77.

Austin, L.G., Bagga, P., 1981. An analysis of fine dry grinding in ball mills. Powder Technol. 28, 83–90.

Austin, L.G., Shah, I., 1983. A method for inter-conversion of Microtrac and sieve size distributions. Powder Technol. 35, 271–278.

Austin, L.G., Klimpel, R.R., Luckie, P.T., 1984. The Process Engineering of Size Reduction: Ball Milling. SME-AIME, New York, pp. 99–110.

Frances, C., Laguerie, C., 1998. Fine wet grinding of an alumina hydrate in a ball mill. Powder Technol., 147–153.

Tangsathitkulchai, C., 2002. Acceleration of particle breakage rates in wet batch ball milling. Powder Technol. 124, 67–75.

Tangsathitkulchai, C., Austin, L.G., 1985. The effect of slurry density on breakage parameters of quartz, coal and copper ore in a laboratory ball mill. Powder Technol. 42, 287–296.

Tangsathitkulchai, C., Austin, L.G., 1988. Rheology of concentrated slurries of particles of natural size distribution produced by grinding. Powder Technol., 293–299.

Tangsathitkulchai, C., Austin, L.G., 1989. Slurry density effects on ball milling in a laboratory ball mill. Powder Technol., 285–293.

Yekeler, M., Ozkan, A., Austin, L.G., 2001. Kinetics of fine wet grinding in a laboratory ball mill. Powder Technol. 114, 224–228.